Effect of heavy doping on the optical properties and band structure of GaAs

František Lukeš,* Sudha Gopalan,† and Manuel Cardona

Max-Planck-Institut für Festkörperforschung, Heisenbergstrasse 1, D-7000 Stuttgart 80, Federal Republic of Germany

(Received 12 June 1992)

We have measured by spectral ellipsometry the pseudodielectric function $\varepsilon(\omega)$ of pure and heavily doped GaAs in the energy range 2–5.5 eV. A dependence of the E_1, $E_1 + \Delta_1$, E_0', and E_2 critical-point energies and the lifetime broadening on doping has been observed. Amplitudes and phase angles for the corresponding critical points were also obtained. A difference between the behavior of n- and p-doped materials was found, especially concerning the magnitudes of critical-point energies and broadening parameters. The results are compared with second-order perturbation-theory calculations of the effect of substitutional impurities on the band structure of GaAs.

I. INTRODUCTION

It is well known that heavy doping influences considerably the physical properties of semiconductors, in particular transport and optical response (see, e.g., Refs. 1 and 2). In this paper we investigate the influence of heavy doping on the linear optical response of both n- and p-type GaAs. For this purpose we have determined the pseudo-dielectric function of these materials in the spectral range from 2 to 5.5 eV at room temperature with the help of spectroscopic ellipsometry.

The influence of doping on the optical properties of GaAs has been discussed by several authors. Cardona, Shaklee, and Pollak[3] observed Burstein-Moss shifts in both n- and p-type GaAs at 297 K with the help of the electroreflectance technique. They reported an increase with doping of the energies of the E_0 and $E_0 + \Delta_0$ peaks observed in the electroreflectance spectra of GaAs samples. An increase with doping was also detected for the so-called E_1 and $E_1 + \Delta_1$ transitions. For other transitions, e.g., E_0', $E_0' + \Delta_0'$, E_2, and $E_2 + \delta$, the peak energies were reported to be essentially independent of the doping level. The authors of Ref. 3, however, did not give a quantitative interpretation of their data. Several additional papers dealing with optical constants of heavily doped GaAs near the absorption edge have also appeared. Sell, and Wecht, for instance,[4] reported the concentration dependence of the refractive index of n- and p-type GaAs between 1.2 and 1.8 eV while Casey, Sell, and Wecht[5] studied the concentration dependence of the absorption coefficient between 1.3 and 1.6 eV. Olego and Cardona[6] investigated photoluminescence in heavily doped p-type GaAs. They found that the dependence of the E_0 energy on the concentration of free holes can be qualitatively described with the help of the expression proposed by Casey and Stern:[7]

$$E_{0,\text{doped}} - E_{0,\text{pure}} = -1.6 \times 10^{-8} p^{1/3}. \tag{1}$$

Quantitatively the results of Ref. 6 are about 50% higher than those in Ref. 7. Vigil, Rodríguez, and Pérez[8] reported reflectance measurements performed at room temperature in the spectral range from 1.2 to 3.8 eV for heavily doped n-GaAs:Te with donor concentration up to 3×10^{18} cm^{-3} and p-type GaAs:Zn with acceptor con-

centration up to 3×10^{19} cm^{-3}. They found that the peaks in the reflectivity spectra corresponding to the E_1 and $E_1 + \Delta_1$ transitions are broadened with increasing doping in both types of samples and shift to lower energies. However, they gave no quantitative treatment or interpretation of their observations.

Since we used the same experimental technique and theoretical considerations as Viña and co-workers used earlier for heavily doped Si and Ge, we do not repeat the details described in Refs. 9–11. Let us only note, however, that in the cases of Si and/or Ge there exist two distinct phenomena pertaining to the effect of doping on direct band edges.

(a) Effects of doping on the lowest band edges, demonstrated, e.g., in the lowest direct transition $\Gamma_8^v \rightarrow \Gamma_6^c$, known as band population effect. They correspond to the Burstein-Moss shift due to the filling of the conduction (valence) band by electrons (holes) in n (p)-type materials. These effects manifest themselves in interband transitions either starting at the top of the valence band for p-type or ending at the bottom of the conduction band in n-type samples. These effects appear also on other direct edges which are not the lowest but involve either transitions starting at the highest point in the valence band in p-type or ending at the lowest point of the conduction band in n-type samples. Besides the Burstein shift, these edges are strongly affected by exchange and correlation involving interaction with the free carriers.[12]

(b) Effects of the interaction with the random impurity potentials on all edges, demonstrated clearly in higher interband transitions which do not start (end) at the top of the valence band (bottom of the conduction band) in the case of p (n) -type semiconductors.

Band calculations often reveal two three-dimensional critical points (CP's) associated with these transitions for either the E_1 or $E_1 + \Delta_1$ gap: a minimum (M_0) at the edge of the Brillouin zone [L point, (π/a) $(1,1,1)$] and a saddle point (M_1) around $(\pi/4a)$ $(1,1,1)$. The separation in energy of each of these two sets of M_0 and M_1 CP's is rather small, probably smaller than the lifetime broadening of the E_1 and $E_1 + \Delta_1$ excitations. Nonlocal pseudopotential calculations, however, shift the M_1 CP close to L thereby eliminating the M_0 CP but still leaving the initial and final bands nearly parallel over a

       ©1993 The American Physical Society

TABLE I. Samples of n- and p-type GaAs used in our measurements. Typical estimated accuracies of the quoted free-carrier concentrations are 20–30 %.

n-type GaAs			p-type GaAs:Zn	
Sample	Dopant	n (cm^{-3})	Sample	p (cm^{-3})
A1		10^{14}	P1	6×10^{18}
A2		10^{16}	P2	1.5×10^{19}
N1	Sn	6×10^{16}	P3	1.6×10^{19}
N2	Sn	1.9×10^{17}	P4	2.5×10^{19}
N3	Se	2.8×10^{17}	P5	3.8×10^{19}
N4	unknown	3.5×10^{17}	P6	7×10^{19}
N5	Se	5×10^{17}	P7	9×10^{19}
N6	Te	1×10^{18}	P8	9.3×10^{19}
N7	Si	3.1×10^{18}	P9	1×10^{20}
N8	Sn	5×10^{18}		
N9	Si	5.2×10^{18}		
N10	Te	5.8×10^{18}		

large region along Λ.[14] It is therefore usual to represent these two CP's by two-dimensional ones. For GaAs these two-dimensional CP's are located at 2.915 eV (E_1) and 3.139 ($E_1 + \Delta_1$).[13,15]

The details of the E_2 transitions are more complicated. In GaAs there exist several CP's which contribute to the E_2 structure.[13] In Si E_2 is ascribed mainly to $\Sigma_2^v \rightarrow \Sigma_3^c$ transitions with $E_2 = 4.33$ eV at about 10 K (Ref. 13) and in Ge to transitions near the $(2\pi/a)$ (0.75,0.25,0.25) point with $E_2 = 4.31$ eV at 5 K. Because of the complex nature of these transitions we may expect some complications when interpreting the results obtained for E_2 transitions in GaAs.[15] A recent theoretical and experimental investigation for $Al_xGa_{1-x}As$ (Ref. 16) attributes the E_2 transitions to a large region of k space in the $\Gamma X U L$ plane [including $(2\pi/a)(0.75, 0.25, 0.25)$] plus a region along the $\{110\}$ directions near the K point.

All p-type samples measured, as well as several n-type samples, were commercial bulk doped. Some of the n-type samples were layers prepared by liquid-phase epitaxy at the MPI, Stuttgart. The dopant concentration was either given by the manufacturer or was taken to be the free-carrier concentration corresponding to the plasma edge obtained from infrared reflectivity measurements. The concentrations and the dopants are summarized in Table I.

In order to obtain the energies of the CP's and their Lorentzian broadening Γ, a line-shape analysis of the experimental data, i.e., ε_1 and ε_2 versus $E = \hbar\omega$, was performed by fitting the numerically obtained second-derivative spectra with respect to the photon energy, i.e., $d^2\varepsilon_1/dE^2$ and $d^2\varepsilon_2/dE^2$, with suitable analytical expressions. The details are discussed in Sec. III.

II. EXPERIMENTAL SETUP

The Zn-doped GaAs samples (p-type) were cut from commercial single crystals. Sn-, Se-, and Te-doped samples (n-type) were grown by liquid-phase epitaxy on GaAs substrates. Sample N7 (Table I) is bulk mate-

rial doped with Si, sample N9 (Si doped) was grown by liquid-phase epitaxy on GaAs substrates.

The bulk samples were mechanically lapped and polished with Al_2O_3 powder. Prior to measurement, they were chemically polished or etched with a bromine-methanol (0.05% Br_2 in methanol) solution.

One p-type sample was mounted and optically aligned in a windowless cell in flowing nitrogen to minimize surface contamination. It was repeatedly etched in situ prior to measurement until the ellipsometric data showed no further changes and the highest values of ε_2 were obtained at energies around that of the E_2 peak. We found that the second derivatives $d^2\varepsilon_1/d^2E$ and $d^2\varepsilon_2/dE^2$ calculated from the data obtained in this way were within experimental error the same as when the sample was placed on the ellipsometer table in air immediately after etching, and remained nearly the same until the next day. Therefore we investigated all other samples only in air while performing the measurements immediately after etching.

The dielectric function spectra $\varepsilon(E) = \varepsilon_1(E) + i\varepsilon_2(E)$ were measured at room temperature between 2.0 and 5.5 eV with an automatic rotating analyzer ellipsometer described in Ref. 9.

III. RESULTS

The experimentally determined ellipsometric parameters Δ and ψ were used to calculate the pseudodielectric functions $\varepsilon_1(E)$ and $\varepsilon_2(E)$ which were not corrected for the presence of an overlayer and/or surface roughness. The data for a pure and a heavily doped p-type GaAs:Zn are shown in Fig. 1. The change of the $\varepsilon_2(E)$ curve of the heavily doped sample with respect to the pure one is qualitatively the same as in the cases of Si (Ref. 9) and Ge:[11] we observed a "redshift" of the peak and a decrease of its magnitude for the heavily doped sample. The maximum value of $\varepsilon_2(E)$ corresponding to the E_1 transitions decreases with doping faster than the maximum of the
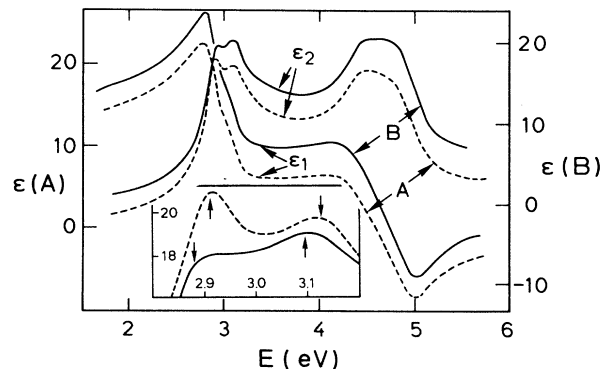

FIG. 1. Solid curves, real (ε_1) and imaginary (ε_2) parts of the pseudodielectric function of bulk GaAs, zinc-doped ($p = 5 \times 10^{19}$ cm^{-3}); dashed lines, the same for an undoped crystal ($n \approx 1 \times 10^{14}$ cm^{-3}). The inset gives a blowup of $\varepsilon_2(\omega)$ in the E_1, $E_1 + \Delta_1$ region in order to display the redshift of the critical points with increasing doping (vertical arrows).
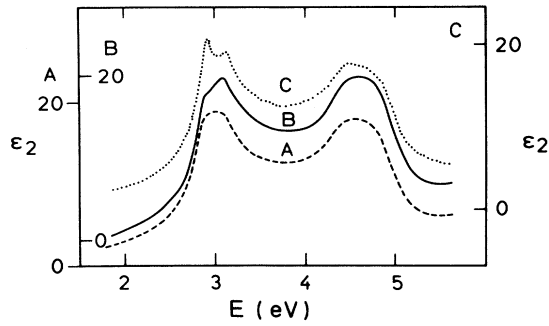
FIG. 2. Imaginary part of the pseudodielectric function ε_2 of GaAs samples: undoped crystals ($n \approx 1 \times 10^{14}$ cm^{-3}), dotted line (C); tin doped ($n = 5.8 \times 10^{18}$ cm^{-3}), solid line (B); epitaxial layer, silicon doped ($n = 5.2 \times 10^{18}$ cm^{-3}), dashed line (A).

$E_1 + \Delta_1$ transitions. Similar effects have been obtained for Ge.[11] Corresponding changes are much smaller for the E_2 transitions, again in agreement with the effects of doping on the E_2 of Si (Ref. 9) and Ge.[11]

The situation is more complicated in n-type GaAs. We found that Si on the one hand and Te, Se, and Sn on the other influence the form of the dielectric functions, especially $\varepsilon_2(E)$, in different ways. Si doping in GaAs leads to a strong supression of the detailed structure of both E_1 and $E_1 + \Delta_1$ peaks when compared with the effect of Sn or Te (Fig. 2).

The slight redshifts of the $\varepsilon_1(E)$ and $\varepsilon_2(E)$ spectra found from the data of Figs. 1 and 2 are clearly seen in the second-derivative spectra of both dielectric functions presented in Figs. 3–6. This shift is characteristic of all heavily doped samples, both n- and p-type, similarly to the cases of Si (Ref. 9) and Ge.[11] The magnitudes of these shifts differ for different transitions and, even more important, for n- and p-type. This last fact contrasts with observations for Si and Ge, for which shifts and broadenings depend only on the transitions at hand and the impurity concentration, but not on the carrier type (donors
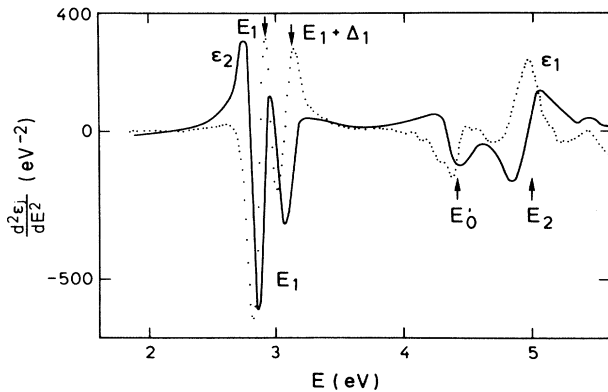

FIG. 3. Second derivatives with respect to the photon energy of the real (ε_1, dotted line) and imaginary (ε_2, solid line) parts of the pseudodielectric function of a tin-doped bulk GaAs crystal with $n = 5.8 \times 10^{18}$ cm^{-3}.

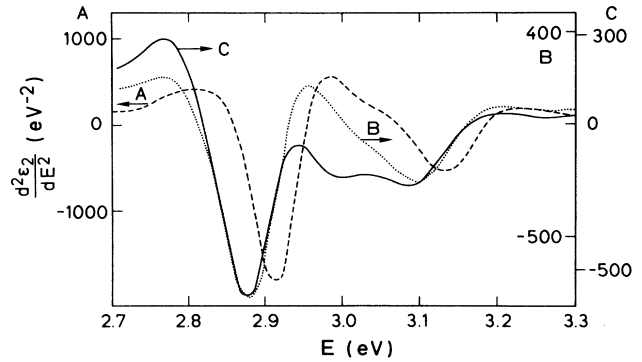FIG. 4. Second derivatives with respect to the photon energy of the imaginary part of the pseudodielectric function (ε_2) of n-type crytals. Pure bulk crystal ($n \approx 1 \times 10^{14}$ cm^{-3}), dashed line (vertical scale A). Epitaxial layers, tin doped ($n = 5 \times 10^{18}$ cm^{-3}), dotted line (B). Silicon doped ($n = 5.2 \times 10^{18}$ cm^{-3}), solid line (C).

or acceptors). The Lorentzian broadening parameter Γ increases with increasing doping, as expected.

The detailed comparison of the second-derivative spectra leads to the following conclusions.

A. E_1 gap

The structures related to the E_1 and $E_1 + \Delta_1$ transitions may be best expressed by two-dimensional critical points (2D CP). We also tried to represent our data by excitonic-type curves for pure samples (i.e., zero-dimensional CP's: Lautenschlager et al.[15] reported that up to about 300 K it is possible to describe the E_1 and $E_1 + \Delta_1$ structures by discrete exciton-type Lorentzians although above 300 K 2D CP's are required). Both types of line shapes led to similar fit quality, considering the quality of the agreement between the model and the experimental spectra for pure samples. Since the spectra of highly doped samples can be represented by a 2D CP (or by a mixture of 2D CP's as expressed by the excitonic phase angle φ) better than with the help of
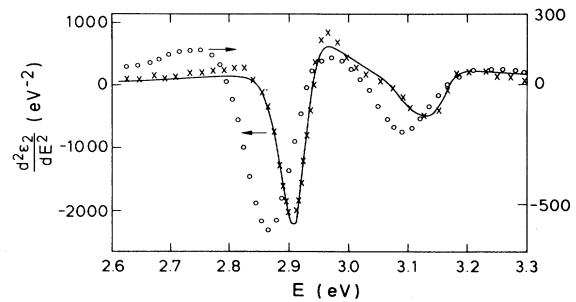

FIG. 5. Second derivatives with respect to the photon energy of the imaginary part of the pseudodielectric function (ε_2). Lightly doped crystal ($n \approx 1 \times 10^{16}$ cm^{-3}): crosses, experiment; solid line, theory. Zinc-doped, bulk crystal ($p = 9.3 \times 10^{19}$ cm^{-3}): open circles, experiment.
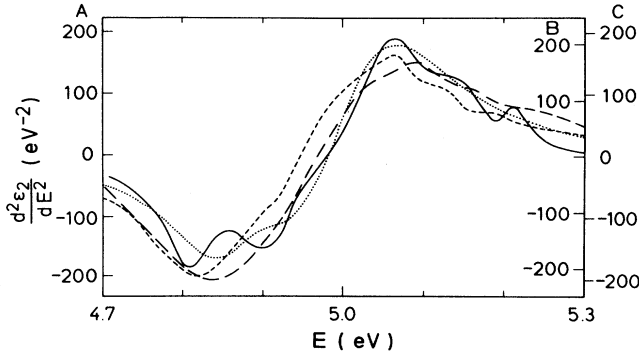
FIG. 6. Second derivatives with respect to photon energy of the measured imaginary part of the pseudodielectric function. Pure crystal ($n \approx 1 \times 10^{14}$ cm^{-3}), solid line (A). Epitaxial layer (Si doped, $n = 5.2 \times 10^{18}$ cm^{-3}), long-dashed line (C). Bulk crystal (Zn-doped, $p = 7 \times 10^{19}$ cm^{-3}), short-dashed line (B). CP fit to the pure crystal data, dotted line.

the discrete excitonic curve, we used 2D CP's as representatives of these structures for all samples in order to be able to compare the line-shape parameters of different samples and to ascertain the dependence of E_1 and $E_1 + \Delta_1$ on doping. The dependence of E_1 and $E_1 + \Delta_1$ on free-carrier concentration is shown in Fig. 7(a) for p-type GaAs and in Fig. 7(b) for n-type GaAs. $\Delta E_1 = E_{1,p} - E_{1,0}$, $\Delta \bar{E}_1 = (E_1 + \Delta_1)_p - (E_1 + \Delta_1)_0$, where the subscript p means the corresponding value of a heavily doped sample while 0 indicates pure samples. Although the magnitudes of ΔE_1 and $\Delta \bar{E}_1$ for p-type GaAs are comparable with those found for Si and Ge, the corresponding changes in n-type GaAs are approximately 4 times larger for $n = 10^{19}$ cm^{-3} (this reference value was obtained by extrapolation from lower concentrations since our most heavily doped n-type GaAs sample had $n = 5.8 \times 10^{18}$ cm^{-3}, see Table II). We found that ΔE_1 and $\Delta \bar{E}_1$ may be expressed as functions of free-carrier
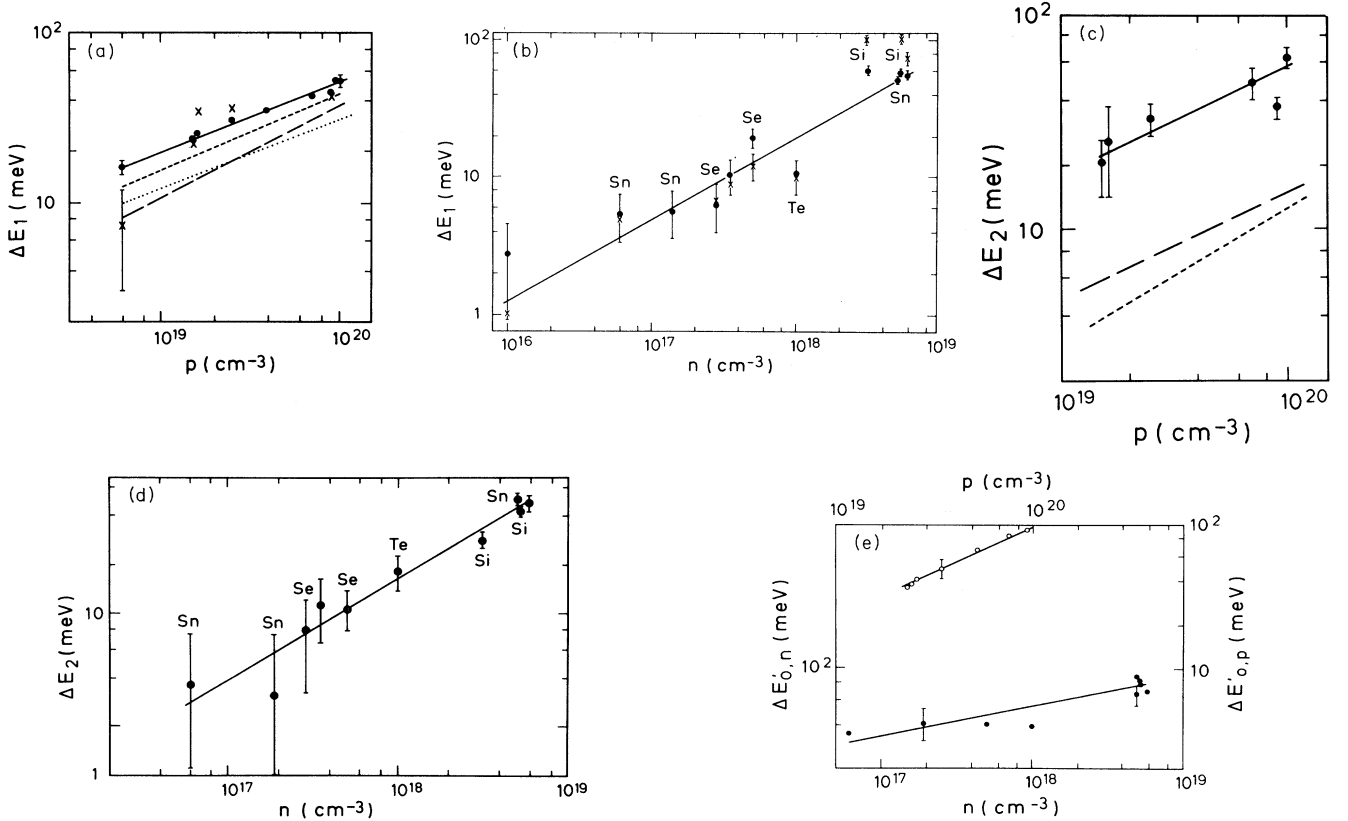

FIG. 7. Dependence on doping concentration of the critical-point energies E_i represented by the redshifts ΔE_i referred to the undoped sample. (a) p-type GaAs:Zn, black dots, ΔE_1; crosses, $\Delta \bar{E}_1 = \Delta(E_1 + \Delta_1)$. The solid line represents the best fit to the experimental data to a p^α law, yielding $\alpha_p = 0.43 \pm 0.04$. The short-dashed line displays theoretical results which lead to $\alpha_p = 0.44$ for critical point (CP) at $\mathbf{k} = (\pi/a)(3/8, 3/8, 3/8)$. The long-dashed line also gives the theoretical results ($\alpha_p = 0.48$) for the CP at $\mathbf{k} = (\pi/a)(1/4, 1/4, 1/4)$ while those for the CP at L [$\mathbf{k} = (\pi/a)(1/2, 1/2, 1/2)$] are represented by the dotted line ($\alpha_p = 0.40$). (b) n-type GaAs, dots, ΔE_1; crosses, $\Delta \bar{E}_1$. Solid line, experiment ($\alpha_n = 0.60 \pm 0.05$). (c) p-type GaAs:Zn, dots, ΔE_2. Solid line, fit to those dots ($\alpha_p = 0.49 \pm 0.08$). Long-dashed line, theory ($\alpha_p = 0.51$, CP at the X point). Short-dashed line, theory [$\alpha_p = 0.58$, CP at $\mathbf{k} = (\pi/a)(3/4, 1/4, 1/4)$]. (d) n-type GaAs, solid circles, E_2. Solid line, fit to the experimental points ($\alpha_n = 0.60 \pm 0.06$). Whenever only one point is shown for a given n or p in (a) and (c) both values of ΔE_1 and $\Delta \bar{E}_1$ are the same. (e) $\Delta E_0'$ for p-type GaAs (Zn-doped). Open circles, experimental data. Solid line, fit to the experimental points ($\alpha_p = 0.53 \pm 0.03$). n-type GaAs: solid circles, experimental data. Solid line, fit to the experimental points ($\alpha_n = 0.21 \pm 0.05$).

TABLE II.   Values of α obtained from fits to the ΔE_i of different band gaps of GaAs with doping concentration (free-carrier concentration) n (p) to n^α or p^α laws. The experimental $\Delta E_{i,n}$ and $\Delta E_{i,p}$ are given for $n = p = 1 \times 10^{19}$ cm^{-3}.

| | α_n[a] | | α_p | | $\Delta E_{i,n}$ | $\Delta E_{i,p}$ |
	Theor.	Expt.	Theor.	Expt.	E (meV)	
ΔE_1	0.5	0.60 ± 0.05	0.40[b]	0.43 ± 0.04	79	20
			0.44[c]			
ΔE_2	0.5	0.60 ± 0.06	0.58[d]	0.49 ± 0.08	72	19
			0.51[e]			
$\Delta E_0'$	0.5	0.21 ± 0.05		0.53 ± 0.03	89	32

[a]Analytical calculation, see Eq. (16).
[b]At $\mathbf{k} = (\pi/a)(1/2, 1/2, 1/2)$.
[c]At $\mathbf{k} = (\pi/a)(3/8, 3/8, 3/8)$.
[d]At $\mathbf{k} = (\pi/a)(3/4, 1/4, 1/4)$.
[e]At $\mathbf{k} = (\pi/a)(1, 0, 0)$.

concentration in the form

$$\Delta E_1 \sim n^\alpha \quad \text{or} \quad p^\alpha, \tag{2}$$

$\alpha_p = 0.43 \pm 0.04$, $\alpha_n = 0.60 \pm 0.05$. It is evident (see Fig. 7) that ΔE_1 and $\Delta \bar{E}_1$ are the same for a given sample within the experimental error, with the exception of the values for both Si-doped samples. For these samples both ΔE_1 and $\Delta \bar{E}_1$ lie clearly above the line representing the $\Delta E_1 \sim n^\alpha$ dependence, $\Delta \bar{E}_1$ being much larger than ΔE_1 for both samples. We have already seen that the pseudodielectric function ε_2 (Fig. 2) and the second derivative of ε_2 with respect to energy (Fig. 4) for Si-doped samples differ from the corresponding curves for Sn-doped crystals with approximately the same carrier concentration. Similar observations have been made for some (but not all) of the remaining critical-point parameters. It is difficult to express quantitatively the dependence of $\Delta\Gamma_1$ (for E_1) and $\Delta\bar{\Gamma}_1$ (for $E_1 + \Delta_1$) with a reasonable degree of confidence [Figs. 8(a) and 8(b)]. If we assume the dependence

$$\Delta\Gamma_1 = \Gamma_{1,\text{doped}} - \Gamma_{1,\text{pure}} \sim n^\alpha \quad \text{or} \quad p^\alpha \tag{3}$$

(and likewise for $\Delta\bar{\Gamma}_1$) then α_n seems to be close to 0.3 for both E_1 and $E_1 + \Delta_1$ transitions in n-type GaAs, but with rather large error bars ($\alpha_n = 0.28 \pm 0.09$). The values of α_p for p-type GaAs are 0.28 ± 0.05 for Γ_1 and 0.28 ± 0.07 for $\Delta\bar{\Gamma}_1$. In p-type GaAs we found systematically lower values for $\Delta\bar{\Gamma}_1$ than for $\Delta\Gamma_1$.

We also were able to determine with reasonable accuracy the angle φ which represents the mixture of contiguous 2D CP's as expressed by the equation

$$\varepsilon = A - \ln\left(E_0 - E - i\hbar\Gamma\right) e^{i\varphi}. \tag{4}$$

In Fig. 9 we plot the dependence of φ on carrier concentration for the E_1 and $E_1 + \Delta_1$ CP's (φ_1), E_0' (φ_0') and E_2 (φ_2). Generally this dependence, if any, is weak. φ_1 is close to $\pi/2$ for both E_1 and $E_1 + \Delta_1$ transitions irrespective of the type of sample, in contrast with the dependence of ΔE_1, $\Delta\bar{E}_1$, and Γ_1, $\bar{\Gamma}_1$ on electron and hole concentrations. The only exceptions are the φ_1 values of Si-doped GaAs which are considerably lower (by about 35°) than $\pi/2$.
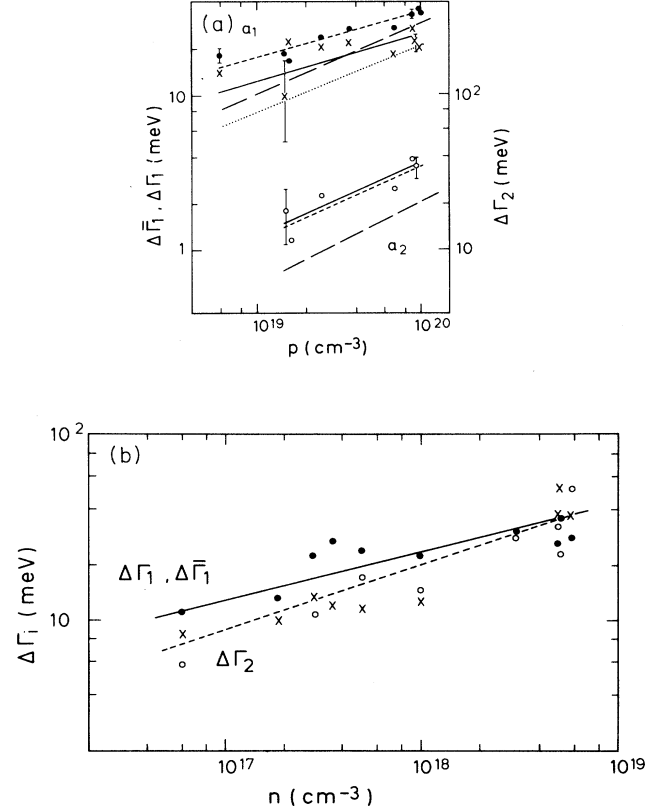

FIG. 8.   Increase in Lorentzian broadening of critical point $\Delta\Gamma_i$ with doping. (a) p-type GaAs (Zn-doped). (a_1)Dots, $\Delta\Gamma_1$. Crosses, $\Delta\bar{\Gamma}_1$. Short-dashed line, fit to the experimental $\Delta\Gamma_1$ ($\alpha_p = 0.28 \pm 0.05$). Solid line, fit to the experimental $\Delta\bar{\Gamma}_1$ ($\alpha_p = 0.28 \pm 0.07$). Long-dashed line, theory [$\alpha_p = 0.47$, CP at $\mathbf{k} = (\pi/a)(1/4, 1/4, 1/4)$]. Dotted line, theory [$\alpha_p = 0.41$, CP at $\mathbf{k} = (\pi/a)(3/8, 3/8, 3/8)$]. ($a_2$) Open circles, $\Delta\Gamma_2$. Solid line, fit to the open circles ($\alpha_p = 0.46 \pm 0.08$). Short-dashed line, theory [$\alpha_p = 0.48$, CP at $\mathbf{k} = (\pi/a)(3/4, 1/4, 1/4)$]. Long-dashed line, theory [$\alpha_p = 0.53$, CP at $\mathbf{k} = (\pi/a)(1, 0, 0)$]. (b) n-type GaAs: solid circles, $\Delta\Gamma_1$. Crosses, $\Delta\bar{\Gamma}_1$. Open circles, $\Delta\Gamma_2$. Solid line, experiment ($\Delta\Gamma_1$), $\alpha_n = 0.28 \pm 0.09$. Short-dashed line, experiment ($\Delta\bar{\Gamma}_1$ and $\Delta\Gamma_2$), $\alpha_n = 0.34 \pm 0.09$.
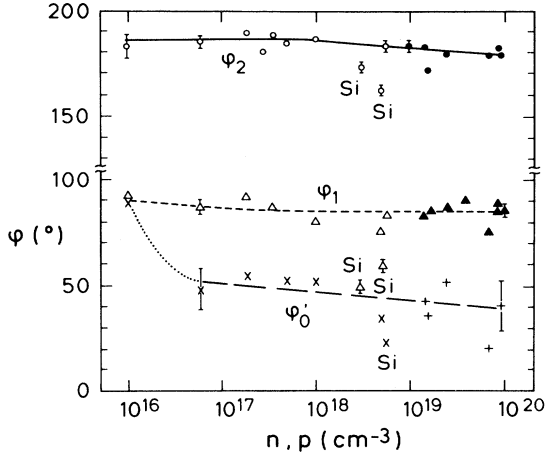
FIG. 9. Dependence on doping of the excitonic parameter φ defined in Eq. (4) for E_1, E_2, and E_0' critical points. Only experimental results are given since no quantitative theory is available. Open circles, triangles, and $\times$ correspond to n-type GaAs; solid circles, triangles, and $+$ correspond to p-type GaAs.

B. E_2 gap

We have already mentioned that the structure of the E_2 transition in GaAs is rather complicated since it is composed of several CP's in different regions of the Brillouin zone having approximately the same energy. We tried several possible fits to the experimentally determined second derivative of the pseudodielectric function near E_2. Our conclusion is that it may be best fitted with a 2D CP, in agreement with Lautenschlager et al.[15] We did not investigate in detail whether this fit is justified from the point of view of the band structure of GaAs (Ref. 16) since this point is not essential for the evaluation of the dependence of E_2 on doping.

It is, however, of questionable value to express the dependence of Γ_2 on doping level since especially this parameter is considerably influenced by the fact that the E_2 region has contributions from several transitions: the separation between these transitions, which may depend on doping, contributes to the fitted value of Γ. In spite of it we find that Γ_2 grows with increasing free-carrier concentration in both n- and p-type GaAs, as expected. Rather surprisingly, φ_2 is constant within the experimental error in the whole free-carrier concentration range, namely, $\varphi_2 = \pi$, which corresponds to a maximum 2D CP. This value agrees within the experimental accuracy with the results.[15]

It is known (see, e.g., Ref. 15) that at room temperature the peak in $\varepsilon_2(E)$ which represents the E_2 transitions is rather broad. The same holds also for the corresponding structure in the second derivative of ε_2 (Fig. 6). In the latter we recognize a weak structure which we found difficult to express with the help of additional critical points, especially for heavily doped samples. Although we succeeded in representing some of the experimental curves, especially those for samples with low carrier concentration, with two CP's we decided to use only

one CP in order to represent the E_2 transitions for *all* our samples. Therefore the accuracy of our results concerning the dependence of E_2, and especially the meaning of the fitted value of Γ_2, on carrier concentration is questionable.

Similarly to the case of the E_1 transitions we fit our experimental results for E_2 with the relation

$$\Delta E_2 \sim n^\alpha \quad \text{or} \quad p^\alpha . \tag{5}$$

We obtained by this procedure $\alpha_n = 0.60 \pm 0.06$ and $\alpha_p = 0.49 \pm 0.08$ [Figs.7(c) and 7(d)]. Hence both α_n and α_p for E_2 are the same, as for E_1, within the experimental accuracy. Moreover, while the data for Si-doped n-type GaAs differ from those characterizing n-type GaAs doped with either Sn, Se, or Te in the case of the E_1 transitions, there is almost no difference for the ΔE_2 and $\Delta \Gamma_2$ values. Also φ_2 is about $13°$ smaller for Si-doped GaAs than for the other samples with the same n or p (Fig. 9), a difference much smaller than found for φ_1 ($\delta\varphi_1 = 35°$). We conclude qualitatively that Si atoms substituting for Ga influence considerably the E_1 band gap (along Λ) while their influence on the band states which contribute to E_2 is smaller than for other donors. Let us note that our φ_1 and φ_2 for undoped samples agree with those given in Ref. 15.

C. E_0' gap

The E_0' structure in undoped Si is ascribed to the $\Gamma_{25'}^v \rightarrow \Gamma_{15}^c$ transition and its energy almost coincides with that of the E_1 transitions [$E_0' = 3.40$ eV, $E_1 = 3.45$ eV at 10 K (Ref. 13)]; in Ge $E_0' = 3.25$ eV at 15 K (Ref. 13) and the E_0' transition is isolated but rather weak. In GaAs $E_0' = 4.488$ eV, corresponding to $\Gamma_8^v \rightarrow \Gamma_7^c$ transitions, while $E_0' + \Delta_0' = 4.659$ eV.[13] E_0' is well separated from the E_2 structure but, especially for highly doped samples at room temperature, we cannot completely neglect the influence of E_2 on E_0' when we try to describe analytically the experimental spectra (second derivatives of ε_1 and ε_2 with respect to energy). This fact complicates the interpretation of our experimental results. When comparing our experimental $d^2\varepsilon_i/dE^2 = f(E)$ ($i = 1, 2$) functions with model line shapes we conclude that 2D CP's represent the data well, in agreement with Ref. 15. Similar to the case of the E_1 and E_2 transitions we attempted to approximate the experimental results with

$$\Delta E_0' \sim n^\alpha \quad \text{or} \quad p^\alpha, \quad \Delta \Gamma_0' \sim n^\alpha \quad \text{or} \quad p^\alpha.$$

This ansatz worked rather well for p-type GaAs but only poorly, if at all, for n-type GaAs. [Fig. 7(e)] The results of our calculation expressed in terms of α_n, α_p (E_0') and α_n, α_p (Γ_0') are summarized in Tables II and III.

IV. THEORY

We use for calculating the influence of doping on the band structure of GaAs the general approach which was successful in the case of Si (Ref. 9) and Ge.[11] It in-

TABLE III. Values of α obtained from fits to the Γ_i's of different band gaps of GaAs vs carrier concentration n (p) with a n^α or p^α law. Experimental $\Delta\Gamma_{i,n}$ and $\Delta\Gamma_{i,p}$ are given for $n = p = 1 \times 10^{19}$ cm^{-3}.

| | α_n^a | | α_p | | $\Delta\Gamma_{i,n}$ | $\Delta\Gamma_{i,p}$ |
	Theor.[a]	Expt.	Theor.	Expt.	E (meV)	
$\Delta\Gamma_1$	0.5	0.28 ± 0.09	0.47[b]	0.28 ± 0.05	42	18
			0.41[c]			
$\Delta\Gamma_2$	0.5	0.34 ± 0.09	0.48[d]	0.46 ± 0.08	46	23
			0.53[e]			
$\Delta\Gamma_0'$	0.5	0.18 ± 0.03		0.88 ± 0.06	98	17

[a]Analytical calculation, see Eq. (16).
[b]At $\mathbf{k} = (\pi/a)(1/2, 1/2, 1/2)$.
[c]At $\mathbf{k} = (\pi/a)(3/8, 3/8, 3/8)$.
[d]At $\mathbf{k} = (\pi/a)(3/4, 1/4, 1/4)$.
[e]At $\mathbf{k} = (\pi/a)(1, 0, 0)$.

volves the evaluation of first- and second-order perturbation terms in the screened impurity potential. Like in the cases of Si and Ge, the first-order perturbation terms can be neglected. This is particularly true of our results since the free-carrier concentration of our most heavily doped sample (GaAs:Zn, $p = 1 \times 10^{20}$ cm^{-3}) is more than one order of magnitude lower than that of the most heavily doped Si and Ge samples. It was concluded in Refs. 9 and 11 that the first-order perturbation term (linearly proportional to the impurity concentration) could only manifest itself for samples with the highest doping levels: this effect was not identified in Ge and Si even for the highest dopings available ($\sim 10^{20}$ cm^{-3}).

The calculation of the second-order perturbation term should be, for GaAs, similar to the case of Si and Ge. The structure of the valence band is very similar to that of Ge, not only qualitatively but also quantitatively (Ge: $m_{hh} = 0.347$, $m_{lh} = 0.042$; GaAs: $m_{hh} = 0.50$, $m_{lh} = 0.076$). The calculation of the effect of acceptors on the gaps of GaAs should thus parallel that for p-type Ge and lead to similar results. The calculation for p-type GaAs was performed numerically; the results are summarized together with experimental data in Tables II and III and in Figs. 7 and 8.

The case of n-type GaAs should, in principle, be easier than that of n-type Ge since the structure of its conduction band is simpler: no near degeneracy of the lowest direct and indirect gaps occurs in GaAs, in contrast to Ge. Also, there is only one absolute minimum at Γ_6^c with a scalar electron effective mass. Let us start with the second-order perturbation term for the shift $\Delta_{\mathbf{k}m}$ of a band energy (l is the band index) [see Ref. 9; Eq. (16)]:

$$\Delta_{\mathbf{k}l} = N_e \sum_{\mathbf{q},m} \frac{|\langle \mathbf{k}n | V^{\text{imp}} | \mathbf{k} + \mathbf{q}, m \rangle|^2}{e_{\mathbf{k}l} - e_{\mathbf{k}+\mathbf{q},m}} \quad (6)$$

with

$$V^{\text{imp}}(q) = \frac{4\pi e^2}{\varepsilon(q)q^2} = \frac{4\pi e^2}{q^2 \left[\varepsilon_L(q) - \frac{4\pi}{Vq^2}\sum_r F_r(q_n^*) \right]}, \quad (7)$$

where N_e is the number of free electrons, $\mathbf{q}$ a wave vector, $\varepsilon_L(q)$ the dielectric function of the pure host semiconductor, $e_{k,l}$ the electron energy, V^{imp} the localized perturbing impurity potential. The Lindhard polarizability $F_r(q_n^*)$ is defined and discussed in Refs. 9 and 11. In the special case of n-type GaAs we obtain

$$V^{\text{imp}}(q) = \frac{4\pi e^2}{q^2\varepsilon_L(q) + \frac{4m_e}{\pi}(3\pi^2 N_e)^{1/3}g(q^*)}, \quad (8)$$

$$g(q^*) = \frac{1}{2}\left\{ 1 - \frac{1}{q^*}\left[1 - \left(\frac{q^*}{2}\right)^2 \right] \right\} \ln\frac{1 - \frac{q^*}{2}}{1 + \frac{q^*}{2}}, \quad (9)$$

where q^* is defined in Ref. 9. The second term in the denominator of Eq. (8) varies very rapidly with q around Γ_6^c (note that $m_e = 0.065$ in GaAs) and contributions with q close to $q = 0$ may dominate since screening is rather weak on account of the small mass. It is thus necessary to use a very fine mesh of q points close to zero in the integration, a fact which complicates the numerical procedure. Hence we made a rough estimate using the following considerations. Neglecting the q dependence of the wave functions we can write

$$\Delta_{\mathbf{k},l} \approx N_e \sum_{\mathbf{q},m} \frac{|V^{\text{imp}}(q)|^2}{e_{\mathbf{k},l} - e_{\mathbf{k}+\mathbf{q},m}}. \quad (10)$$

We want to find out how $\Delta_{\mathbf{k},n}$ scales with N_e. We have

$$V^{\text{imp}}(q) = \frac{4\pi e^2}{q^2 + \kappa^2}, \quad (11)$$

where

$$\kappa^2 = \frac{4m_e}{\pi}(3\pi^2 N_e)^{1/3} g(q^*). \quad (12)$$

$g(q^*)$ depends only weakly on q and we can assume that κ^2 is independent of q. The following approximation is then found:

$$\Delta_{\mathbf{k},l} \sim N_e \sum_{\mathbf{q},n} \left(\frac{4\pi e^2}{q^2 + \kappa^2} \right) \frac{1}{e_{\mathbf{k},l} - e_{\mathbf{k}+\mathbf{q},m}}. \quad (13)$$

Around a band extremum related to a critical point:

$$e_{\mathbf{k},l} - e_{\mathbf{k+q},m} \approx -\frac{\hbar^2 q^2}{2m^*} , \qquad (14)$$

where m^* is an average effective mass. Therefore

$$\Delta_{\mathbf{k},l} \sim N_e \sum_{\mathbf{q}} \left(\frac{1}{q^2 + \kappa^2}\right)^2 \frac{1}{q^2}. \qquad (15)$$

We transform the summation in (15) into an integral and find (let us denote $N_e = n$)

$$\Delta_{\mathbf{k},l} \sim \frac{n}{\kappa^3}.$$

In view of the relation between κ and n contained in Eq. (8) we come to the conclusion that

$$\Delta_{\mathbf{k},l} \sim n^{1/2}. \qquad (16)$$

Hence the slope in the dependence of $\ln \Delta E_i$ on n (see Fig. 7) is calculated to be $\alpha_n = 0.5$ when only intermediate states near the Γ_6^c minimum are taken into account. In view of the crudeness of the assumption involved in Eq. (14) we believe that $\alpha = 0.5$ is in reasonable agreement with the experimental values for E_1 and E_2 listed in Table II ($\simeq 0.6 \pm 0.06$). The experimental value for E_0' ($\alpha \simeq 0.21 \pm 0.05$) is however considerably smaller.

V. DISCUSSION

When comparing the results found for Si (Ref. 9) and especially for Ge (Ref. 11) with the present data for GaAs there appear some common features but also some noticeable differences. The common features concern the qualitatively similar dependence of ΔE_i and $\Delta \Gamma_i$ on doping concentration and the possibility of expressing both effects with the help of the same semiempirical relations, namely, $\Delta_i \sim p^\alpha$ or n^α, $\Delta \Gamma_i \sim p^\alpha$ or n^α. The most significant difference is that in GaAs the experimental values of both ΔE_i and $\Delta \Gamma_i$ differ considerably for n- and p-type samples. Especially, the magnitudes of ΔE_i and $\Delta \Gamma_i$ at the carrier concentrations n or $p = 1 \times 10^{19}$ cm^{-3} differ remarkably, as displayed in Tables II and III. They are larger for n-type than for p-type samples.

The blurring of the E_1 peak, especially with respect to $E_1 + \Delta_1$, is more pronounced in n-type samples even at much lower impurity concentrations than in p-type ones and at concentrations 1–2 orders of magnitude lower than for Ge (Ref. 11) (compare our Figs. 1 and 2 with Fig. 1 in Ref. 11). The difference is not so large for the second derivative $d^2\varepsilon/dE^2$ (compare our Figs. 4 and 5 with Fig. 2 in Ref. 11). Particularly interesting is the case of n-type GaAs doped with Si (we had two samples of this sort, see Table I, both giving the same qualitative results) where E_1 and $E_1 + \Delta_1$ peaks are indistinguishable on the ε_2 curve (Fig. 2). Also the second derivatives $d^2\varepsilon^2/dE^2$ of Si-doped GaAs differ in the region of $E_1 + \Delta_1$ peak considerably from that of pure GaAs and the n-type GaAs doped with Sn with almost the same free-electron concentration (Fig. 4). The reason for this difference

is not clear. Contrary to the case of Ge,[11] where the blurring of the E_1 peak was accompanied by a decrease of the φ_1 angle (which represents the amount of excitonic interaction in the E_1 structure, see Fig. 3 in Ref. 11), in the case of GaAs φ_1 depends only weakly, if at all, on free-carrier concentration irrespective of whether the sample is n- or p-type. The φ_1 value is close to 90° except for Si-doped samples, which means that, at least at room temperature, the E_1 transition has the character of an almost pure 2D saddle point.

Our experimental data for p-type GaAs in the region of E_1 and $E_1 + \Delta_1$ transitions agree best with an assignment to the Λ region centered at $\mathbf{k} = (\pi/a)(3/8, 3/8, 3/8)$, as demonstrated in Table II. At $\mathbf{k} = (\pi/a)(1/2, 1/2, 1/2)$ we find considerably worse agreement between theory and experiment and for $\mathbf{k} = (\pi/a)(1/4, 1/4, 1/4)$ the calculated α is 0.48 and $\Delta E_{1,\exp}/\Delta E_{1,\text{theory}} = 2$ ($p = 1 \times 10^{19}$ cm^{-3}).

For the E_2 transition we performed the calculation at $\mathbf{k} = (\pi/a)(3/4, 1/4, 1/4)$ and $\mathbf{k} = (\pi/a)(1, 0, 0)$. For ΔE_2 we obtained slightly better agreement with experiment for $\mathbf{k} = (\pi/a)(1, 0, 0)$ [see Fig. 7(c)] while for $\Delta \Gamma_2$ agreement is clearly better when the calculations are performed at $\mathbf{k} = (\pi/a)(3/4, 1/4, 1/4)$ [see Fig. 8(a)]. While this is not wholly satisfactory, it is not surprising in view of the rather complicated structure of the E_2 transitions.[15] We may thus conclude that our results are compatible with the interpretation of Lautenschlager et al.[15] who assigned the E_2 transition in GaAs predominantly to the region around $\mathbf{k} = (\pi/a)(3/4, 1/4, 1/4)$.

It is difficult to comment on the E_0' transitions. While we can represent the experimental curves with a 2D CP, large scattering between calculated curves and experimental points is obtained. The dependence $\Delta E_{0,p}'$ on p seems to be reasonable [Fig. 7(e)] but $\Delta E_{0,n}' = f(n)$ gives the physically unreasonable result $\alpha_n = 0.21 \pm 0.05$ [α should lie between 1/3 and 1 (Refs. 11 and 17)].

In spite of the fact that they found some difference between calculated values of α for n- and p-type Ge, Viña and Cardona[11] could not detect any such difference in the experimental results. On the other hand, there are considerable differences for n- and p-type GaAs. We have demonstrated here that differences are found not only for the α values but also for the ΔE_1 at a specific carrier concentration $n = p$ (see Table II). The same is true for $\Delta \Gamma_i$ (Table III). Unfortunately, the impurity concentrations of our n- and p-type samples do not overlap, the highest n being lower than (but comparable to) the lowest p value. Nevertheless we have been able to establish that ΔE_i and $\Delta \Gamma_i$ of n-type GaAs at $n = p = 1 \times 10^{19}$ cm^{-3} is about 3–4 times larger than those for p-type GaAs. Rather surprisingly, the values of φ and A (not given here) expressed as functions of n and p result in smooth, monotonic lines. A comment concerning the difference between the effects of Si and those of other n-type dopants is in order. We have repeatedly obtained such differences, in particular consistent results were obtained for epitaxial and for bulk Si-doped samples. Our results are also in agreement with data for heavily Si-doped samples recently published by Snyder and Xiong.[19] Nevertheless the lack of a basic understanding of those differences suggests that they should

be treated with caution. Systematic measurements on more samples for several surface treatments and oxide thicknesses are required in order to confirm or refute such effects. In this respect we mention that differences between the effects of As and P on the dielectric function of Si reported in Ref. 18 were shown to result from surface conditions by Aspnes, Studna, and Kinsbron.[20]

Note added in proof. The results reported here for E_1 and $E_1 + \Delta_1$ may be slightly affected by the Franz-Keldysh effect induced by the surface electric field. Experiments to ascertain this contribution are in progress [M. K. Kelly (private communication)]. The effect of acceptor passivation with deuterium on the elliposometric spectra has been recently reported [P. de Mierry and M. Stutzmann, Phys. Rev. B **46**, 13 142 (1992)].

*Present address: Dept. of Solid State Physics, Faculty of Science, Masaryk University, Kotlarska 2, 611 37, Brno, Czechoslovakia.

†Present address: Rue des Flamands 1, CH-2525 Le Landeron, Switzerland.

[1] M. Cardona, in *Solid State Physics*, edited by F. Seitz, D. Turnbull, and H. Ehrenreich (Academic, New York, 1969), Suppl. 11.

[2] B.I. Shklovskii and A.L. Efros, *Electronic Properties of Doped Semiconductors* (Springer, New York, 1984).

[3] M. Cardona, K.L. Shaklee, and F.H. Pollak, Phys. Rev. **154**, 696 (1967).

[4] D.D. Sell, H.C. Casey, and K.W. Wecht, J. Appl. Phys. **45**, 2650 (1974).

[5] H.C. Casey, D.D. Sell, and K.W. Wecht, J. Appl. Phys. **46**, 250 (1975).

[6] D. Olego and M. Cardona, Phys. Rev. B **22**, 886 (1980).

[7] H.C. Casey and F. Stern, J. Appl. Phys. **47**, 631 (1976).

[8] E. Vigil, J.A. Rodríguez, and R. Pérez Alvarez, Phys. Status Solidi B **90**, 409 (1978).

[9] L. Viña and M. Cardona, Phys. Rev. B **29**, 6739 (1984).

[10] L. Viña, S. Logothetidis, and M. Cardona, Phys. Rev. B **30**, 1979 (1984).

[11] L. Viña and M. Cardona, Phys. Rev. B **34**, 2586 (1986).

[12] See papers by E.O. Kane, in *Solid State Electronics,* edited by P. T. Landsberg (Pergamon, Oxford, 1985), Vol. 28, p. 3; F. Berggren and B.E. Sernelius, *ibid.*, p. 11; S.T. Pantelides *et al.*, *ibid.* p. 17.

[13] Landolt-Börnstein Tabellen, New Series, Group III, Vol. 23, Pt. a, edited by A. Goldmann and E. E. Koch (Springer, Heidelberg, 1989).

[14] J.R. Chelikowski and M.L. Cohen, Phys. Rev. B **14**, 556 (1976).

[15] P. Lautenschlager, M. Garriga, S. Logothetidis, and M. Cardona, Phys. Rev. B **35**, 9174 (1987).

[16] S. Logothetidis, M. Alouani, M. Garriga, and M. Cardona, Phys. Rev. B **41**, 2959 (1992).

[17] L. Viña, Ph.D. thesis, University of Stuttgart, 1984.

[18] G.E. Jellison, Jr., F.A. Modine, C.W. White, R.F. Wood, and R.T. Young, Phys. Rev. Lett. **46**, 1414 (1981).

[19] P.G. Snyder and Y.M. Xiong, Surf. Interf. Anal. **18**, 107 (1992).

[20] D.E. Aspnes, A.A. Studna, and E. Kinsbron, Phys. Rev. B **29**, 768 (1984).